

Photoresponsivity Enhancement of SnS-Based Devices Using Machine Learning and SCAPS Simulations [†]

Abdelhak Maoucha ¹, Faycal Djéffal ^{1,*}, Tarek Berghout ² and Hichem Ferhati ^{1,3}

¹ LEA, Department of Electronics, University of Batna 2, Batna 05000, Algeria; email1@email.com (A.M.); email2@email.com (H.F.)

² Laboratory of Automation and Manufacturing Engineering, University of Batna 2, Batna 05000, Algeria; email2@email.com

³ ISTA, University of Larbi Ben M'hidi, Oum El Bouaghi 04000, Algeria

* Correspondence: faycal.djeffal@univ-batna2.dz

[†] Presented at the 10th International Electronic Conference on Sensors and Applications (ECSA-10), 15–30 November 2023; Available online: <https://ecsa-10.sciforum.net/>.

Abstract: In this work, we propose a novel alternative design technique based on combined SCAPS numerical simulations and Machine Learning (ML) computation to improve the photocurrent performances for efficient eco-friendly optoelectronic applications. In this context, a new SnS absorber structure based on introducing gold (Au) nanoparticles (NPs) is proposed. It is revealed that the proposed design framework can predict the best spatial distribution of Au NPs allowing enhanced optical behavior of SnS absorber film. This can pave the way for the optoelectronic systems designers to identify the geometry and the appropriate material for each layer of the device. Moreover, the results of the proposed SnS-based structure offer an innovative approach for the elaboration of eco-friendly high-efficiency thin-film optoelectronics devices that is more promising than the previously reported designing techniques.

Keywords: photocurrent; photosensing; machine learning; tin-sulfide; efficiency

1. Introduction

Photodetectors hold a prominent role in optoelectronic devices as they possess the capacity to convert optical signals into electrical signals. They find applications in various fields, including early missile threat detection, optical communication, environmental monitoring, water purification, flame detection, ultraviolet astronomy, environmental surveillance, remote sensing, biomedicine, and photography [1–3]. In this circumstance, various materials like perovskites, monolayers, colloidal quantum dots, and solution-processable substances have been extensively investigated with the goal of addressing the primary challenges associated with conventional photodetectors [3–5]. Particularly, tin sulfide (SnS) stands out as a highly promising material. It is characterized by its non-toxic properties, chemical stability, Earth abundant, high carrier mobility, visible light-absorption ability, low recombination velocity, and a tunable direct bandgap [6,7]. These attributes collectively position SnS as an exceptional candidate for high-performance optoelectronic devices. In addition, tin sulfide encompasses various phases, including SnS, Sn₂S₃, SnS₂, Sn₃S₄, and Sn₄S₅, each characterized by distinct stoichiometric ratios of tin and sulfur. The synthesis and doping of these diverse SnS phases are achievable through various methods, such as pulse electrodeposition (PED), spray pyrolysis, physical vapor deposition (PVD), plasma-enhanced chemical vapor deposition (PECVD), chemical bath deposition (CBD), electron beam evaporation (EBM), atomic layer deposition (ALD), and RF magnetron sputtering [6–10]. While certain SnS photodetectors have exhibited noteworthy performance, their achieved results still fall short of expectations. Moreover, the SnS

Citation: Maoucha, A.; Djéffal, F.; Berghout, T.; Ferhati, H. Photoresponsivity Enhancement of SnS-Based Devices Using Machine Learning and SCAPS Simulations. *Eng. Proc.* **2023**, *56*, x. <https://doi.org/10.3390/xxxxx>

Academic Editor(s): Name

Published: 15 November 2023



Copyright: © 2023 by the authors. Submitted for possible open access publication under the terms and conditions of the Creative Commons Attribution (CC BY) license (<https://creativecommons.org/licenses/by/4.0/>).

alloys are not free from some disadvantages. One of which is their low resistance to the aggressive influence of environmental factors such as temperature, oxygen and electromagnetic radiation. With that, there are new different classes of Sulfide-based materials with good electronic properties have been developed using appropriate experimental facilities [11,12]. To address this challenge, noble metal nanoparticles can be introduced in the SnS absorber layer. This can enhance the photodetector optoelectronic properties through improving light absorption and generating plasmonic effects. Nonetheless, in the domain of thin film semiconductor devices, a persistent iterative optimization process results in the inefficient utilization of energy and material resources, leading to elevated experimental costs and increased human labor demands. Intuitively, to expedite the experimentation timeline and reduce the overall cost, machine learning (ML) analysis techniques can be a potential solution. The field of machine learning analysis has gained prominence as a powerful tool for addressing challenges. It resides within the domain of artificial intelligence and is instrumental in uncovering latent insights within datasets. Machine learning can extract a diverse range of authentic material information through computational and data mining methodologies. In this work, employing ML analysis, we accurately predict the plasmonic impact on optoelectronic properties by optimizing the positioning of gold nanoparticles within the SnS layer (top, middle, or bottom) and determining the most suitable nanoparticle radius to achieve optimal performance. The outcomes reveal that our eco-friendly SnS photodetector design, featuring gold nanoparticles, significantly enhances its optoelectronic characteristics, establishing it as a promising choice for the development of cost-effective and environmentally friendly photodetectors.

2. Device Structure and Modeling Frameworks

2.1. Device Structure

The proposed SnS absorber film consists of introducing Au NPs as shown in Figure 1a. The latter shows a cross sectional view of the investigated SnS absorber and the spatial distribution of the introduced Au NPs is depicted in Figure 1b. From this figure, P denotes the NPs position from the surface following the z direction, r is the nanoparticle radius and S refers to the spacing between Au NPs. The proposed SnS absorber film is considered on a glass substrate and the thin-film thickness (t_{SnS}) is fixed at 400 nm. It is to note that the chemical stability of the investigated structure including Au NPs was already investigated and demonstrated by several published works [7,13,14].

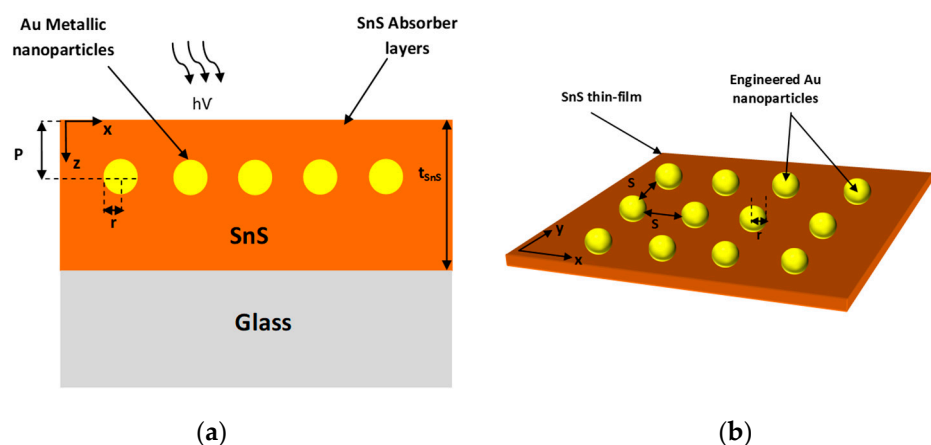


Figure 1. (a) Cross-sectional view of plasmonic gold nanoparticles based on the SnS Absorber film (b) schematic of SnS surface decorated Au NPs.

2.2. Modeling Frameworks

In the initial phase of our study, we utilize the SCAPS (Solar cell Capacitance Simulator) application to generate an extensive dataset [15]. Before that, Finite Difference Time

Domain method (FDTD) is used to estimate the absorbance of the proposed SnS thin-film based on specially distributed Au NPs. The details regarding the optical modeling of the proposed SnS absorber layer decorated with Au NPs can be found in our previous work [4]. Subsequently, in the second phase, we employ machine learning-based calculations to forecast the influence of the position and radius of gold nanoparticles on the optoelectronic properties of the SnS photodetector. The ML model has been trained using our SCAPS-based calculation database. Correlation analysis and machine learning algorithms have been exploited to investigate the key parameters affecting the optical behavior of SnS absorber film. SCAPS-ML predictive approach has been developed to determine the best spatial distribution of Au NPs, offering fast and crucial guidance for experimental elaboration of SnS-based optoelectronic devices with high-photodetection capabilities.

3. Results and Discussion

Figure 2 shows the variation of the photocurrent as a function of the NPs radius for the proposed SnS-based photodetector. It can be seen from this figure that the introduction of Au NPs leads to enhance the device optical behavior, where enhanced photocurrent is achieved as compared to the conventional SnS thin-film. This improvement can be attributed to the role of introducing Au NPs in enhancing light management in the SnS absorber layer through generating plasmonic effects. Besides, the highest photocurrent ($I_{ph} = 21$ mA) is achieved for the specific Au NPs radius of 25 nm. It can be also revealed from Figure 2 that the use of higher radius values leads to decreasing the device photocurrent. This indicates the complex optical behavior of SnS absorber film when Au NPs are introduced, where their geometry and spatial distribution can greatly affect the film optical properties. This opens up new insights for the implementation of ML analysis techniques to study and understand the effect of Au NPs plasmons on the photodetection capabilities of SnS photodetectors.

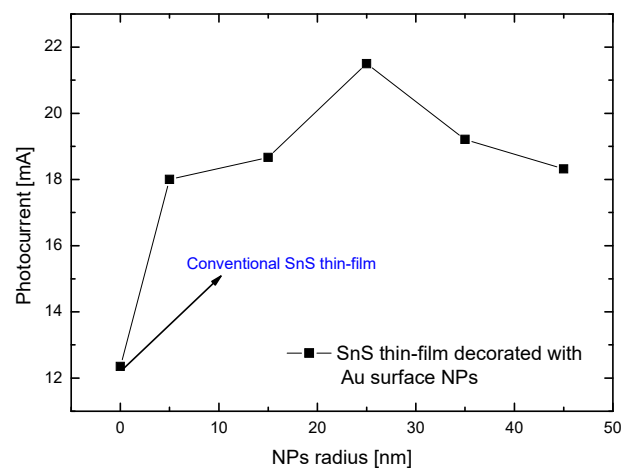


Figure 2. Variation of the photocurrent as a function of the Au NPs radius.

In the context of machine learning modeling, and since the collected data contains an amount of observations of 138 samples, which appears to be a light volume feature space, a simple data visualization will be effective in providing guidance on feature selection and model selection as well. Accordingly, Figure 3 deals with both inputs (subfigures (a,b)) and outputs (subfigure (c)) of the dataset. First, the photocurrent variation shows a kind of monotonicity in the deterioration by demonstrating a kind of regular degradation behaviors over time. Similarly, such patterns can also be distinguished in the NPs positions. Whereas NPs Radius exhibit a sort of periodicity that corresponds neither to inputs nor

outputs. In this case, a first look at feature selection strongly suggests eliminating these unnecessary features, which definitely leads to model bias. Second, variations in NPs positions and photocurrent over time show clear behavior of data drift. This means that this type of data is subject to continuous change in its characteristics making the model generalization able to be out-of-date if one not considering such issue.

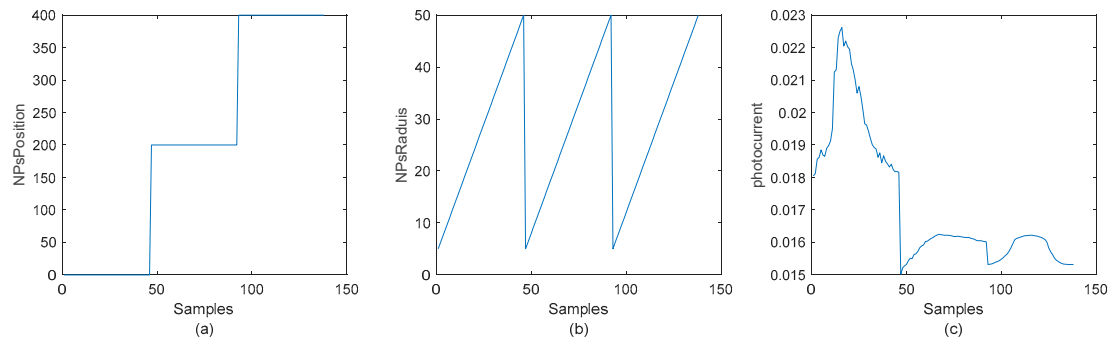


Figure 3. Dataset features: (a,b) inputs; (b) output.

In this work, suggestions for overcoming these challenges are twofold. First, the data is subjected to a feature selection process including only NPs positions features. After that, these features are also made subject to normalization layer via min-max scaling in the range [0, 1]. Second, adaptive learning rules are also integrated to ensure that the model is continually updated with new data and overcomes data drift issues. In this case, data drift problems are addressed by involving a neural network with long-short term memory (LSTM) as in [16,17]. It is worth mentioning that the network hyperparameters are manually tuned based on a simple error-trial basis, as in Table 1. Meanwhile, a 3-fold cross-validation technique is used to ensure the stability and generalizability of the model on the data set.

Table 1. List of obtained hyperparameters.

Hyperparameters	Assigned Values
Maximum number of epochs	300
Mini-batch size	30
Neurons	20
Learning algorithm	Adam optimizer
Initial learning rate	0.01
Gradient threshold	1
L2 regularization	0.0001

The model is evaluated according to a robust criterion that includes different estimation error measures, namely root mean squared error (RMSE), root mean of squares (RMS), mean absolute error (MAE). In addition, the learning model is also subject to another performance evaluation criterion represented by R^2 . Simply put, the three errors should approach “zero”, while the R^2 , should approach the value 1 for better model performance. It is worth mentioning that the application of these evaluation criteria was carried out based on a validation set for each learning fold. This guarantees both the approximation capacity and the generalizability of the learning models. Additionally, another comparative study between the proposed architect and an ordinary multilayer perceptron (MLP) is also conducted. The comparison conclusions obtained will be very effective in observing the benefits of adaptive learning. An important point to consider in such a case is that the MLP uses the same hyperparameters to ensure a fair comparison.

The obtained results are summarized in Table 2. The cross-validation results of RMSE, MSE and MAE show a way too far and better stability of LSTM compared to ordinary MLP. Additionally, the mean values and standard deviation also explain this important information. This performance gap explains the need to use adaptive learning on the one hand and also the importance of feature selection on the other hand. Furthermore, the results obtained regarding R^2 clearly prove the explain ability and importance of the predictions obtained.

Table 2. Performances evaluation results.

LSTM				
Crossvalidation Folds	RMSE	MSE	MAE	R ²
1	9.49e-4	9.00e-07	6.85e-4	0.72
2	1.03e-3	1.07e-06	7.10e-4	0.75
3	1.25e-3	1.56e-06	9.16e-4	0.65
Average	1.07e-3	1.18e-06	7.7e-4	0.71
Standard deviation	4.91e-4			0.051
MLP				
Crossvalidation folds	RMSE	MSE	MAE	R ²
1	2.09e-3	4.40e-06	1.63e-3	-0.36
2	1.65e-3	2.74e-06	1.31e-3	0.382
3	1.37e-3	1.89e-06	1.12e-3	0.58
Average	1.71e-3	3.01e-06	1.35e-3	0.20
Standard deviation	8.11e-04			0.5003

4. Conclusions

In this paper a new computation framework based on combined Scaps numerical simulations and machine learning has been developed. The proposed approach can predict rapidly and accurately the photosensing of SnS based sensor including plasmonic effects and the impact of the gold nanoparticles position and size. Applying LSTM learning rules to such a data drift and complexity problem allows the learning model to be updated based on any changes in the data. This is explained by great performance in approximation metrics such as RMSE, MSE and MAE. Meanwhile, R^2 clearly demonstrates the importance of the results from aexpandability perspective. As for the prospects, this work will continue to explore such a tool for more complex and massive data, to reach more generalized conclusions in the context of data complexity and drift.

Author Contributions: Conceptualization, A.M., F.D., T.B. and H.F.; methodology, F.D.; validation, H.F., T.B. and F.D.; formal analysis, H.F., T.B. and F.D.; investigation, H.F., T.B. and F.D.; data curation, H.F., T.B. and F.D.; writing—original draft preparation, F.D. and T.B.; writing—review and editing, H.F., T.B. and F.D.; All authors have read and agreed to the published version of the manuscript.

Funding: This research received no external funding.

Conflicts of Interest: The authors declare no conflict of interest.

References

1. Kawamura, F.; Song, Y.; Murata, H.; Tampo, H.; Nagai, T.; Koida, T.; Imura, M.; Yamada, N. Tunability of the bandgap of SnS by variation of the cell volume by alloying with A.E. elements. *Sci. Rep.* **2022**, *12*, 7434.
2. Drissi, L.B.; Ramadan, F.Z.; Ferhati, H.; Djeflal, F.; Kanga, N.B. New highly efficient 2D SiC UV-absorbing material with plasmonic light trapping. *J. Phys. Condens. Matter* **2020**, *32*, 025701.
3. Ferhati, H.; Djeflal, F. High-Responsivity MSM Solar-Blind UV Photodetector Based on Annealed ITO/Ag/ITO Structure Using RF Sputtering. *IEEE Sensors J.* **2019**, *19*, 7942–7949.
4. Djeflal, F.; Ferhati, H.; Benyahia, A.; Dibi, Z. Performance analysis of SnS photodetector using strained SnO₂ stacked layer: Numerical simulation and DFT calculations. *Microelectron. Eng.* **2023**, *273*, 111961.

5. Zhang, H.; Li, H.; Yu, H.; Wang, F.; Song, X.; Xu, Z.; Wei, D.; Zhang, J.; Dai, Z.; Ren, Y.; et al. High responsivity and broadband photodetector based on SnS₂/Ag₂S heterojunction. *Mater. Lett.* **2023**, *330*, 133037–133037.
6. Dong, W.; Lu, C.; Luo, M.; Liu, Y.; Han, T.; Ge, Y.; Xue, X.; Zhou, Y.; Xu, X. Enhanced UV–Vis photodetector performance by optimizing interfacial charge transportation in the heterostructure by SnS and SnSe₂. *J. Colloid Interface Sci.* **2022**, *621*, 374–384.
7. Ye, Z.; Yu, H.; Wei, J.; Xie, Y. Direct observation of kinetic characteristic on SnS-based self-powered photodetection. *J. Lumin.* **2023**, *253*, 119473–119473.
8. Kacha, K.; Djeflal, F.; Ferhati, H.; Foughali, L.; Bendjerad, A.; Benhaya, A.; Saidi, A. Efficiency improvement of CIGS solar cells using RF sputtered TCO/Ag/TCO thin-film as prospective buffer layer. *Ceram. Int.* **2022**, *48*, 20194–20200.
9. Trukhanov, S.V.; Bodnar, I.V.; Zhafar, M.A. Magnetic and electrical properties of (FeIn₂S₄)_{1-x}(CuIn₅S₈)_x solid solutions. *J. Magn. Magn. Mater.* **2015**, *379*, 22–27.
10. Bodnar, I.V.; Jaafar, M.A.; Pauliukavets, S.A.; Trukhanov, S.V.; Victorov, I.A. Growth, optical, magnetic and electrical properties of CuFe_{2.33}In_{9.67}S_{17.33} single crystal. *Mater. Res. Express* **2015**, *2*, 085901.
11. Zdorovets, M.V.; Kozlovskiy, A.L.; Shlimas, D.I.; Borgekov, D.B. Phase transformations in FeCo–Fe₂CoO₄/Co₃O₄-spinel nanostructures as a result of thermal annealing and their practical application. *J. Mater. Sci. Mater. Electron.* **2021**, *32*, 16694–16705.
12. Migas, D.B.; Turchenko, V.A.; Rutkauskas, A.V.; Trukhanov, S.V.; Zubar, T.I.; Tishkevich, D.I.; Trukhanov, A.V.; Skorodumova, N.V. Temperature induced structural and polarization features in BaFe₁₂O₁₉. *J. Mater. Chem. C* **2023**, *11*, 12406–12414.
13. Troyanchuk, I.O.; Trukhanov, S.V.; Szymczak, H.; Baerner, K. Effect of oxygen content on the magnetic and transport properties of Pr_{0.5}Ba_{0.5}MnO_{3-γ}. *J. Phys.: Condens. Matter.* **2000**, *12*, L155–L158.
14. Kozlovskiy, A.; Egizbek, K.; Zdorovets, M.V.; Ibragimova, M.; Shumskaya, A.; Rogachev, A.A.; Ignatovich, Z.V.; Kadyrzhanov, K. Evaluation of the efficiency of detection and capture of manganese in aqueous solutions of FeCeO_x nanocomposites doped with Nb₂O₅. *Sensors* **2020**, *20*, 4851.
15. Ferhati, H.; AbdelMalek, F.; Djeflal, F. Improved PCE in stable lead-free perovskite solar cells based on band engineering of ETL and absorber. *Sol. Energy* **2023**, *262*, 111805.
16. Berghout, T.; Benbouzid, M.; Amirat, Y. Towards Resilient and Secure Smart Grids against PMU Adversarial Attacks: A Deep Learning-Based Robust Data Engineering Approach. *Electronics* **2023**, *12*, 2554. <https://doi.org/10.3390/electronics12122554>.
17. Berghout, T.; Mouss, M.-D.; Mouss, L.-H.; Benbouzid, M. ProgNet: A Transferable Deep Network for Aircraft Engine Damage Propagation Prognosis under Real Flight Conditions. *Aerospace* **2022**, *10*, 10. <https://doi.org/10.3390/aerospace10010010>.

Disclaimer/Publisher’s Note: The statements, opinions and data contained in all publications are solely those of the individual author(s) and contributor(s) and not of MDPI and/or the editor(s). MDPI and/or the editor(s) disclaim responsibility for any injury to people or property resulting from any ideas, methods, instructions or products referred to in the content.